electronics

MDPI

Article

Selected Aspects of Positioning with the GNSS Galileo

Milan Džunda, Sebastián Čikovský * and Lucia Melníková

Department of Air Traffic Management, Faculty of Aeronautics, Technical University of Kosice, 040 01 Kosice, Slovakia; milan.dzunda@tuke.sk (M.D.); lucia.melnikova@tuke.sk (L.M.)
* Correspondence: sebastian.cikovsky@tuke.sk

Abstract: The quality of Galileo system services is affected by the accuracy of distance determination from the user's application to the individual satellite. The goal of our research was to find out what influence the accuracy of distance determination between the user's application of the Galileo system and the cooperating satellites of the Galileo system has on the ability to determine the location of the user's application. A solution based on Groebner's algebraic approaches was used to determine the receiver user's position. When creating distance measurement error models between the Galileo system user's receiver and cooperating satellites, we assumed that the values of those errors considered all factors that affected the accuracy of those distance measurements. To evaluate the algorithms, we used a statistical set of 500 simulation results to determine the positioning of the user's application of the Galileo system. If the distances between the user's application and the individual satellite were measured accurately, then the user's application coordinate errors had values between 1.86×10^{-9} m and -1.8×10^{-8} m. These errors should be equal to zero. The positioning error was caused by a numerical error in the calculation due to the software used. If the errors of distance determination from the user's application to the individual satellite varied from -0.05 m to 0.09 m, then the error in determining the positioning of the user's application of the Galileo system was from 0.0 m to 1.2 m. If the distances of the user's receiver to the satellites were measured with errors greater than 0.09 m, the errors in determining its position were much larger. The simulation results confirmed the known fact that the satellites' geometry influences the accuracy of determining the location of the user's application. In the following research, we will solve the problem of how to reduce the sensitivity of the mentioned algorithms when determining the position of the satellite navigation system receiver due to errors in determining the distance from the user's application to the individual satellite.

Keywords: GNSS Galileo; measurement of distance; positioning accuracy

check for updates

Citation: Džunda, M.; Čikovský, S.; Melníková, L. Selected Aspects of Positioning with the GNSS Galileo. *Electronics* **2024**, *13*, 4769. https://doi.org/10.3390/electronics13234769

Academic Editors: Jiajia Chen, Ying Xu and Ming Gao

Received: 31 October 2024
Revised: 25 November 2024
Accepted: 29 November 2024
Published: 2 December 2024

Copyright: © 2024 by the authors. Licensee MDPI, Basel, Switzerland. This article is an open access article distributed under the terms and conditions of the Creative Commons Attribution (CC BY) license (https://creativecommons.org/licenses/by/4.0/).

1. Introduction

The accuracy of distances determination from the user's application to the individual satellite significantly affects the Galileo system's quality of service. It is obvious to recognize that technological progress and innovation in the processing of Galileo measurement signals can contribute to the positioning accuracy of Galileo users. It is, therefore, necessary to continuously address the distance determination process from the user's application to the individual satellite. Paying attention to the processing of the measured results is also required.

Previous papers analyzed issues and challenges related to providing a safe and reliable global navigation system and new opportunities, perspectives, and trends in satellite navigation [1,2]. The authors paid attention to the interference of measurement signals, synchronization, signal manipulation (spoofing), and unauthorized forwarding of signals (meaconing). The effect of errors in determining distances from the user's application to the individual satellite, atmospheric delay, and multipath propagation of measurement GNSS signals on the accuracy of determining the position of the GNSS user is stated

in [3,4]. The authors state that these factors directly translate into user positioning errors. The authors' analysis in [5] showed that factors such as high-gain antennas, powerful processors, and low internal receiver noise contribute to more accurate receiver-to-satellite distance measurements. The effectiveness of corrections in determining the position of a satellite navigation system user's receiver depends mainly on accurate measurements of the distances from the user's application to the individual satellite [6]. Even small errors in these measurements can lead to inaccurate positioning after corrections are applied. In [7], the performance of RTK (real-time kinematic) and PPP (precise point positioning) techniques to achieve accurate positioning using GNSS receivers is compared. The authors state that RTK achieves higher accuracy but requires a nearby reference station. PPP offers a more flexible approach without a reference station but may have lower accuracy. Research conducted in [8–10] suggests that the geometry of satellites, the interference and monitoring interference in GNSS operation, including methods for detection and recognition, significantly impact the accuracy of determining the location of system users. Works [11–13] provide some insights from monitoring interference over an extended period in the L-band and on the E6 spectrum. Frequent interference has been observed in this band due to radars. The authors of these papers emphasize the necessity of a thorough investigation of the impact of jamming on navigation systems, especially when the jamming signals are high-power. The research in [14] examines the influence of interference on global navigation satellite systems. It focuses on the recently developed multiplexed binary offset carrier (MBOC) modulation in Galileo E1 civil signals. Using simulation results, the authors assess and discuss the impact of continuous-wave interference (CWI) on the Galileo E1 civil signal. The effectiveness of real-time accurate positioning with a single-frequency signal using Galileo satellites was evaluated in [15,16]. The results confirmed that Galileo was more accurate than GPS. The benefits of the GNSS Galileo E6 signal are presented in [16]. The authors highlight the potential of E6 signals of GNSS systems in the developing commercial services in the European Union. The analysis in [17] aims to investigate GSSN Galileo's reliability for three years. The results indicate a direct correlation between the accuracy and reliability of GNSS Galileo and its constellation. Contributions [18,19] are devoted to the initial phase of the high accuracy service (HAS) in connection with Galileo. Its complex structure, architecture, and initial operational efficiency are presented. The authors assess the capabilities of GNSS Galileo. The research's focus, the notes of which are presented in [20], was to compare GNSS Galileo, GPS, and GLONASS. GNSS Galileo demonstrated high precision and fast convergence. Paper [21] characterizes the performance of the Galileo HAS product in a static and road scenario characterized by decimeter accuracy in poor visibility. Methods for suppressing interference in GPS, GLONASS, GALILEO, and BeiDou navigation signals using advanced filtering algorithms and adaptive antenna arrays are presented in [22]. The effectiveness of these techniques has been evaluated through simulations and real experiments, enabling further research on optimizing GNSS signal processing. As part of the study [23], an interference detector was designed and implemented to identify interfering GNSS signals. The design results in a flexible receiver, providing accurate positioning. The positioning performance in the maritime environment using signals from different GNSS in the Gulf of Finland is listed in [24]. The authors present an advanced stochastic GNSS model for position calculation. This model is suitable for a marine GNSS receiver. In work [25], the authors state that the Bancroft method could be one method for calculating the position of the GNSS receiver. Possibilities for determining the receiver's position of the global navigation satellite system user based on Groebner's algebraic approaches are listed in [26]. The authors of this work present equations for calculating the position of the satellite navigation system user's receiver using the range-measuring method.

Telemetry for a relative navigation system design is analyzed in [27,28]. The studies' authors designed a system for the navigation of flying objects that operate in a telecommunication network and use a telemetry method to determine their position. They also evaluated the positioning accuracy of flying objects depending on the characteristics of the

telecommunication network and the accuracy of distance measurement between different network users.

The Galileo system uses two basic principles to determine the position of the receiver: measuring the distance or the signal's phase. Our research goal was to find out how measuring $d_{i\text{-}E}$, i = 1–4, affects the accuracy of determining the position of an unknown object P (see Figure 1). The accuracy of the Galileo system was evaluated using the telemetry method and based on Groebner's algebraic approaches.

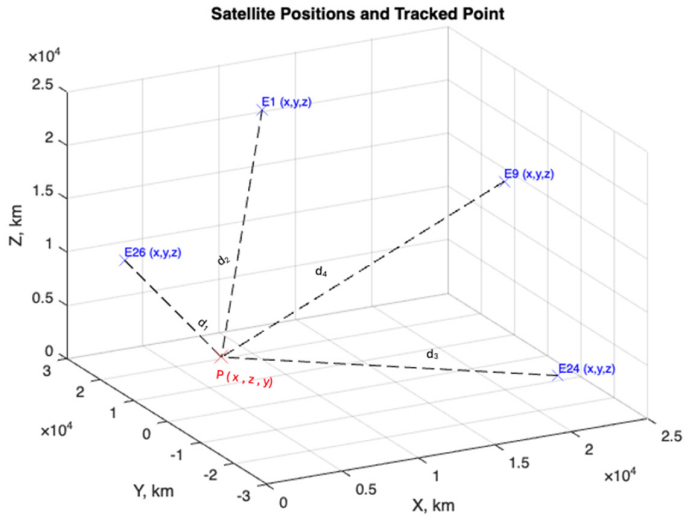


Figure 1. Positions of the Galileo system satellites and the user's receiver in the geocentric coordinate system. Variant number 1.

2. Materials and Methods

This section describes the methodology of creating selected models used in GNSS Galileo to determine the position of the user's receiver. We also obtained equations with which we determined the position of the GNSS Galileo user's application and verified its accuracy. An analysis of the influence of the constellation of GNSS Galileo satellites on the precision of determining the position of the user's receiver was also performed.

2.1. Selecting the Location of the User's GNSS Galileo Receiver and Satellites

Next, we will present the essence of positioning using the Galileo system. In Figure 1, we present the positions of the Galileo satellites (E26, E24, E9, and E1) at UTC 05:30:12 pm, 31 December 2023.

The coordinates of the individual satellites and the reference point are written down in Table 1.

Table 1. Coordinates of Galileo system satellites and the user's receiver. Variant number 1.

Name	X, m	Y, m	Z, m
GSAT0203 (E26)	3,377,247.0	28,079,223.0	8,771,714.0
GSAT0205 (E24)	21,180,560.0	−20,423,644.0	3,104,781.0
GSAT0209 (E9)	20,007,875.0	−9,754,554.0	19,510,975.0
GSAT0210 E1	9,391,888.0	14,368,898.0	24,119,456.0
ARP KSC +300.0 m	3,934,235.0	1,529,238.0	4,766,291.0

Satellite positions are shown in blue, and the Galileo P system user (receiver) is in red. The distances between point P (x,y,z) and the individual satellites are marked di, i = 1–4.

Point P (Galileo GNSS user) is above the Košice airport reference point, at a height of 300 m above this point.

Assume that the position of the Galileo system satellites (x_i, y_i, z_i), where i = 1 to 4 and the distances d_{i-E} are known. We can then calculate position point P (x,y,z). We determine the position of P based on the solution of equations with three unknowns. The distances $d_{i\text{-}E}$, i = 1,2,3,4, are determined according to the equation:

$$d_{i-E} = \sqrt{(x - x_i)^2 + (y - y_i)^2 + (z - z_i)^2}, \text{where i} = 1 \text{ to } 4. \quad (1)$$

As a rule, the satellite's time base (clock) and the user's receiver are not synchronous. This fact may cause errors in the determination of d_{i-E}. We assume that the satellite is broadcasting the data at time t_{iE}. Let t_{pE} be the time of receiving this message. The following applies to the value of d_{i-E}:

$$d_{i-E} = c(t_{pE} - t_{iE}) = c \cdot \tau_{iE}, \text{where c is the speed of light, i} = 1 \text{ to } 4. \quad (2)$$

The d_{i-E} distances can be loaded with many errors, so they are referred to as pseudo-distances. Therefore, d_{i-E} is a pseudo-distance. We write the shift of the receiver's clock by Δt as a distance as follows:

$$b = c \cdot \Delta t. \quad (3)$$

We express the distance D_{i-E} like this:

$$D_{i-E} = d_{i-E} - b, \quad (4)$$

where i = 1 to 4, d_{i-E} is the pseudo-distance, D_i is the true distance, and b is measurement inaccuracy. The time Δt is proportional to the synchronization error.

For the position of user P, we apply:

$$(d_{i-E} - b) = c \cdot (\tau_{i-E} - \Delta t) = \sqrt{(x - x_i)^2 + (y - y_i)^2 + (z - z_i)^2}, \quad (5)$$

where i = 1 to 4.

We modify relation (5) as follows:

$$(x - x_i)^2 + (y - y_i)^2 + (z - z_i)^2 - (-b + d_{i_E})^2 = 0, \text{ where i} = 1 \text{ to } 4, \quad (6)$$

x, y, z is the location of user's P,
x_i, y_i, z_i are the coordinates of the satellite,
$d_{i\text{–}E}$ is the distance from the user's receiver to satellites,
τ_i is the time that is proportional to the distance of the satellite from the user's receiver,
$\Delta\, t$ is the shift of the receiver's and satellite's time bases,
b is the distance proportional to the shift of the time bases of the receiver and the satellite.

2.2. Algorithms for Determining the Coordinates of the Receiver

The coordinates of receiver P are equal to [26]:

$$(x - x_1)^2 + (y - y_1)^2 + (z - z_1)^2 - (-b + d_{1-E})^2 = 0, \quad (7)$$

$$(x - x_2)^2 + (y - y_2)^2 + (z - z_2)^2 - (-b + d_{2-E})^2 = 0, \quad (8)$$

$$(x - x_3)^2 + (y - y_3)^2 + (z - z_3)^2 - (-b + d_{3-E})^2 = 0, \quad (9)$$

$$(x - x_4)^2 + (y - y_4)^2 + (z - z_4)^2 - (-b + d_{4-E})^2 = 0, \quad (10)$$

where $d_{1\text{–}E}$, $d_{2\text{–}E}$, $d_{3\text{–}E}$, and $d_{4\text{–}E}$ are the distances from the Galileo satellites to the user's receiver,

x_1, y_1, z_1 are the coordinates of GALILEO E26,
x_2, y_2, z_2 are the coordinates of GALILEO E24,

x_3, y_3, z_3 are the coordinates of GALILEO E9,
x_4, y_4, z_4 are the coordinates of GALILEO E19,
x, y, z are the coordinates of the receiver of the Galileo system user,
b is the shift of the user's receiver time base converted to distance.

Modifying Equations (10) and (7), we obtain [26]:

$$f_{14} = x_{14}x + y_{14}y + d_{14}b + e_{14} \tag{11}$$

Modifying Equations (10) and (8), we obtain [26]:

$$f_{24} = x_{24}x + y_{24}y + z_{24}z + b_{24}b + e_{24} \tag{12}$$

Modifying Equations (10) and (9), we obtain [26]:

$$f_{34} = x_{34}x + y_{34}y + z_{34}z + d_{34}\,b + e_{34} \tag{13}$$

This way, we obtain relations for three unknowns based on (11)–(13). In the following calculation, we used the method of multi-polynomial resultants [28].

Functions $f_{1–3}$ have the shape [26]:

$$f_1 = (x_{14}x + d_{41}b + e_{14})\,k + y_{14}y + z_{14}z, \tag{14}$$

$$f_2 = (x_{24}x + d_{42}b + e_{24})\,k + y_{24}y + z_{24}z, \tag{15}$$

$$f_3 = (x_{34}x + d_{43}b + e_{34})\,k + y_{34}y + z_{34}z. \tag{16}$$

Let k be the homogenization factor. Then Jacobi's determinant for x (14)–(16) has a shape [26]:

$$\mathbf{J}_x = det\begin{pmatrix} \frac{df_1}{dy} & \frac{df_1}{dz} & \frac{df_1}{dk} \\ \frac{df_2}{dy} & \frac{df_2}{dz} & \frac{df_2}{dk} \\ \frac{df_3}{dy} & \frac{df_3}{dz} & \frac{df_3}{dk} \end{pmatrix} \tag{17}$$

Functions $f_{4–6}$, for the y coordinate, have the shape [26]:

$$f_4 = (y_{14}y + d_{41}b + e_{14})\,k + x_{14}x + z_{14}z \tag{18}$$

$$f_5 = (y_{24}y + d_{42}b + e_{24})\,k + x_{24}\,x + z_{24}z, \tag{19}$$

$$f_6 = (y_{34}y + d_{43}b + e_{34})\,k + x_{34}x + \,z_{34}z. \tag{20}$$

Then Jacobi's determinant for y (18)–(20) has a shape [26]:

$$\mathbf{J}_y = det\begin{pmatrix} \frac{df_4}{dx} & \frac{df_4}{dy} & \frac{df_4}{dk} \\ \frac{df_5}{dx} & \frac{df_5}{dy} & \frac{df_5}{dk} \\ \frac{df_6}{dx} & \frac{df_6}{dy} & \frac{df_6}{dk} \end{pmatrix} \tag{21}$$

Functions $f_{7–9}$, for the z coordinate, have the shape [26]:

$$f_7 = (z_{14}z + d_{41}b + e_{14})\,k + x_{14}x + \,y_{14}y, \tag{22}$$

$$f_8 = (z_{24}z + d_{42}b + e_{24})\,k + x_{24}x + \,y_{24}y, \tag{23}$$

$$f_9 = (z_{34}z + d_{43}b + e_{34})\,k + x_{34}x + y_{34}y. \tag{24}$$

Then Jacobi's determinant for z (22)–(24) has a shape [26]:

$$\mathbf{J}_z = det \begin{pmatrix} \frac{df_7}{dx} & \frac{df_7}{dy} & \frac{df_7}{dk} \\ \frac{df_8}{dx} & \frac{df_8}{dy} & \frac{df_8}{dk} \\ \frac{df_9}{dx} & \frac{df_9}{dy} & \frac{df_9}{dk} \end{pmatrix} \quad (25)$$

We calculated the determinants $\mathbf{J}x$, $\mathbf{J}y$, and $\mathbf{J}z$ from Expressions (17), (21), and (25). Subsequently, we insert expressions for x, y, and z into Equation (7) and obtain a quadratic function [26]:

$$\mathrm{Ab}^2 + \mathrm{Bb} + \mathrm{C} = 0 \quad (26)$$

Equation (26) has two roots: b+ as P (x+, y+, z+) and b− as P ($x-$, $y-$, $z-$). We obtain a satisfactory solution by calculating the norm [26]:

$$norm = \sqrt{\mathrm{x}^2+\mathrm{y}^2+\mathrm{z}^2}, \quad (27)$$

The correct solution will be the one for which the standard has a value close to the earth's radius [28]. We do not present detailed calculations according to Equations (11) to (27) for better readability of the article.

Utilizing the algorithms (1)–(27), a simulation of the Galileo system's ability to determine the user's receiver position was conducted. We investigated how the accuracy of determining the point P changes depending on the accuracy of the $d_{i\text{-}E}$ measurement. To replicate the errors of the $d_{i\text{-}E}$ distance measurements, 12 generators of normally distributed numbers with a mean value of 0 and a mean square deviation of 1 were employed. These generators were instrumental in simulating the errors of the coordinates ΔXi, ΔYi, and ΔZi, i = 1–4, of the Galileo system satellites. The magnitude of the errors of the coordinates of individual satellites ΔXi, ΔYi, and ΔZi, i = 1–4, was determined by the constant k, which was used to scale the output values of 12 generators of random numbers x_{g_i}, y_{g_i}, and z_{g_i}, i = 1–4. For instance, the expression of the errors ΔX_i is as follows:

$$\Delta X_i = x_{gi} \cdot l \quad (28)$$

The mean value and the mean square deviation of errors ΔXi are equal to:

$$m_{\Delta X_i} = m_{xgi} \cdot l, \mathrm{i} = 1\text{–}4, \quad (29)$$

$$\sigma^2_{\Delta X_i} = \sigma^2_{xgi} \cdot l, \mathrm{i} = 1\text{–}4, \quad (30)$$

where m_{xgi} and σ^2_{xgi} are the mean value and the mean square deviation of the random numbers from the output of the generator, respectively.

We added the generated coordinate errors ΔX_i, ΔY, and ΔZ_i to the exact coordinates of the satellites. We express the imprecise coordinates of the Xin satellites as follows:

$$X_{\mathrm{in}} = X_i + \Delta, i = 1\text{–}4. \quad (31)$$

By relations (1) and (31), we calculated the pseudo-distances of user P to individual satellites d_{i-E} :

$$d_{i-E} = \sqrt{(x - x_{in})^2 + (y - y_{in})^2 + (z - z_{in})^2}, \text{where i} = 1-4. \quad (32)$$

The distance measurement errors of user P to individual satellites Δd_{i-E} are equal to:

$$\Delta d_{i-E} = d_{i-E} - D_{i-E}, \mathrm{i} = 1, 2, 3, 4. \quad (33)$$

The flowchart of the calculation according to algorithms (1) to (33) is listed in Figure 2. First, the satellites' coordinates were entered, and then, using the constant l, random errors were generated in the coordinates of the Galileo system satellites ΔX_i, ΔY_i, and ΔZ_i, i = 1–4 according to the relationship (28). Based on these errors, the fictitious position of each satellite was calculated, and the $d_{i–E}$ pseudo-distances were determined according to relationship (32). The exact $D_{i–E}$ distances from the receiver to the satellites were determined according to the entered accurate coordinates for the satellites and point P. Subsequently, errors were generated measuring the distance Δd_{i-E} according to relationship (33). Then, the position of the user's receiver P(x,y,z) according to the relationships (7) to (27) was determined. Errors in determining the position of the user's coordinates P(x,y,z) were determined by comparing his exact coordinates P(x,y,z) and the calculated coordinates x_c, y_c, and z_c according to relations (7) to (27):

$$\Delta x = x - x_c; \Delta y = y - y_c; \Delta z = z - z_c, \tag{34}$$

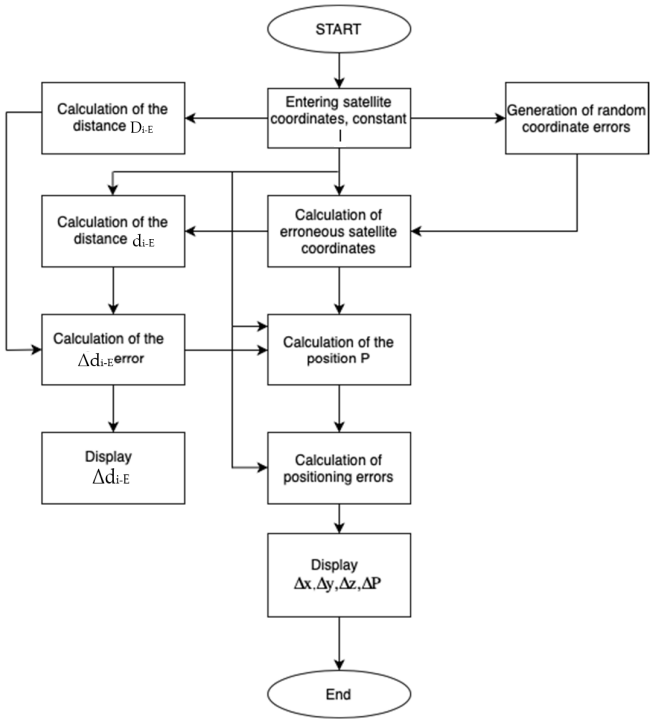


Figure 2. Simulation procedure.

The error in determining the position of the user's ΔP (x,y,z) was determined by comparison of the actual and calculated positions of the user's receiver:

$$\Delta P(x,y,z) = (\Delta x^2 + \Delta y^2 + \Delta z^2)^{0.5}. \tag{35}$$

The results obtained were recorded graphically.

3. Results and Discussion

Through simulation, we verified the accuracy of the created algorithms. To evaluate the derived algorithms, we used a statistical set consisting of 500 simulation results of determining the position of the user's receiver. These results determined the monitored parameters' mean values and mean square deviations. Further, we will present only the essential results of our research so that the article is clear and understandable. We set the constant k equal to 0 and therefore $d_{i-E} = D_{i-E}$. The mean values of m_Δ and the mean square deviations of errors σ_Δ^2 for determining the coordinates of user P for this case are shown in Table 2.

Table 2. Accuracy of user's receiver coordinate calculation for k = 0.

Name	ΔX, (m)	ΔY, (m)
m_Δ, (m)	-1.86×10^{-8}	-8.64×10^{-9}
σ_Δ^2, m^2	0.0	0.0

The results presented in Table 2 show that Equations (1) to (33) are correct. The error values shown in Table 2 were caused by a numerical error in the calculation due to the software used. Furthermore, we checked the appropriateness of the mentioned procedure for different values of constant k. Figures 3–15 show the results of the calculations.

We checked how the errors Δd_{i-E} affect the calculation positions of the user's receiver. The errors Δd_{i-E} were simulated using Equations (28) to (34). The distance determination errors were random for each satellite.

We changed the constant l from 0.01 to 5. The simulation results for l = 0.02 are shown in Figure 3. If l = 0.02, the errors Δd_{i-E} varied from -0.05 m to 0.09 m.

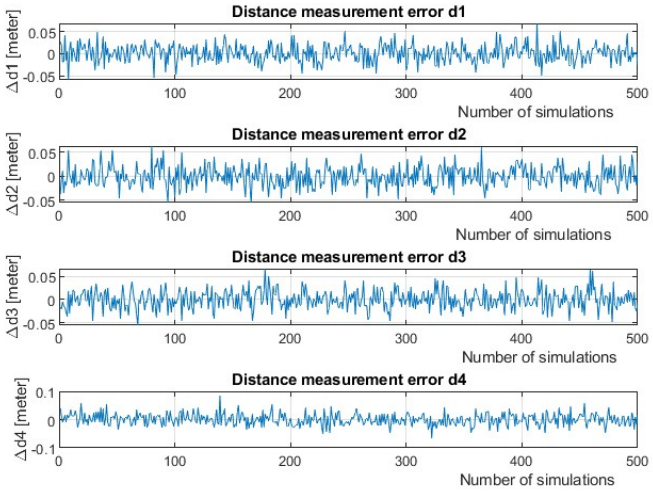


Figure 3. Distance measurement errors Δd_{i-E} for l = 0.02.

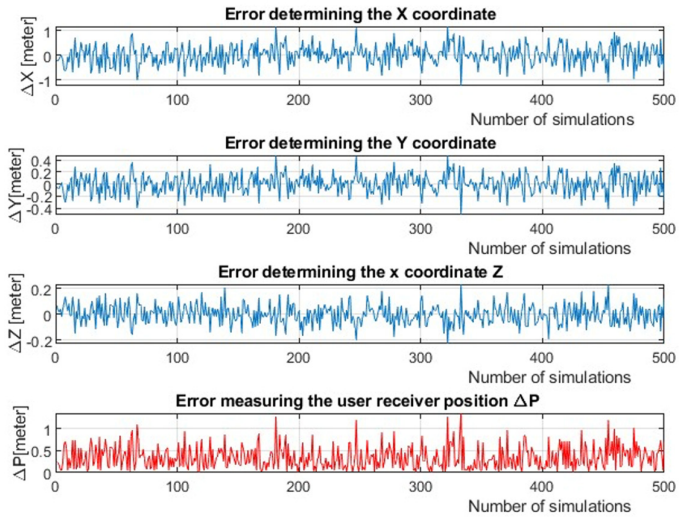


Figure 4. Errors of coordinates ΔX, ΔY, ΔZ, and position ΔP of the user's receiver for l = 0.02.

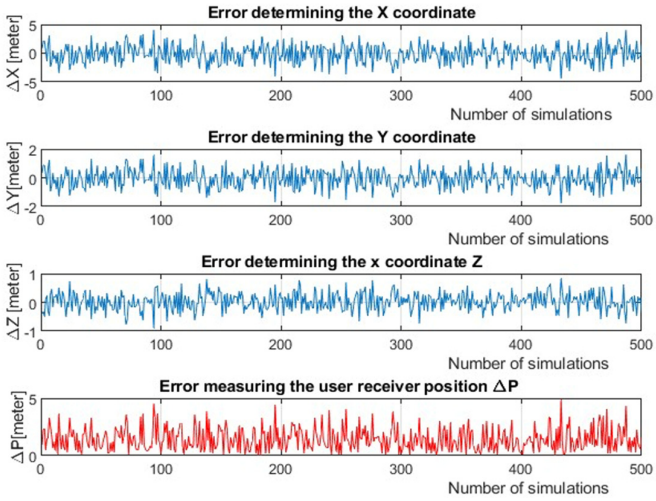


Figure 5. Errors of coordinates ΔX, ΔY, ΔZ, and position ΔP of the user's receiver for l = 0.08.

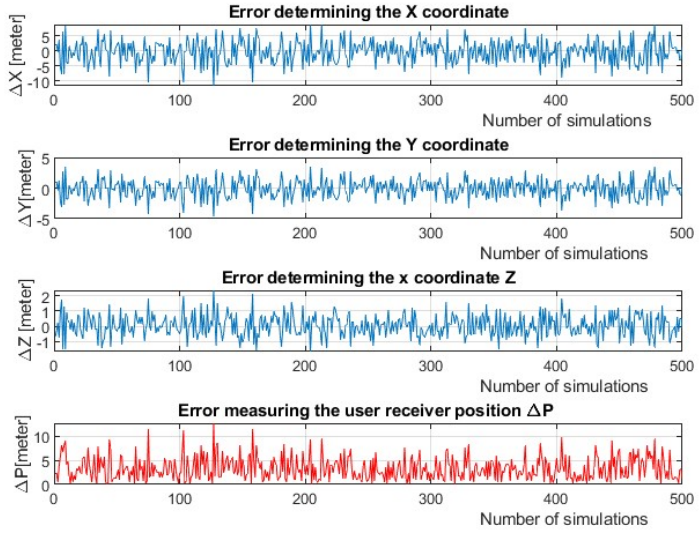


Figure 6. Errors of coordinates ΔX, ΔY, ΔZ, and position ΔP of the user's receiver for l = 0.2.

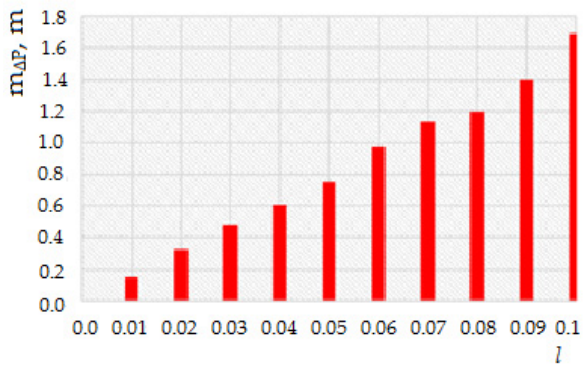


Figure 7. The MVs of the receiver's PDEs $m_{\Delta P}$ depend on the constant l.

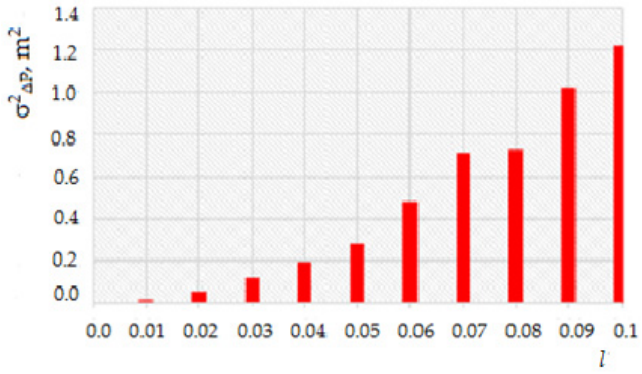


Figure 8. The MSD of the receiver's PDEs $\sigma^2{}_{\Delta P}$ depends on the constant l.

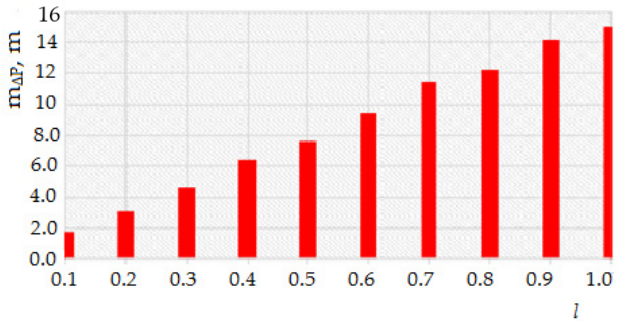


Figure 9. The MVs of the receiver's PDEs $m_{\Delta P}$ depend on the constant l = 0.1 to 1.0.

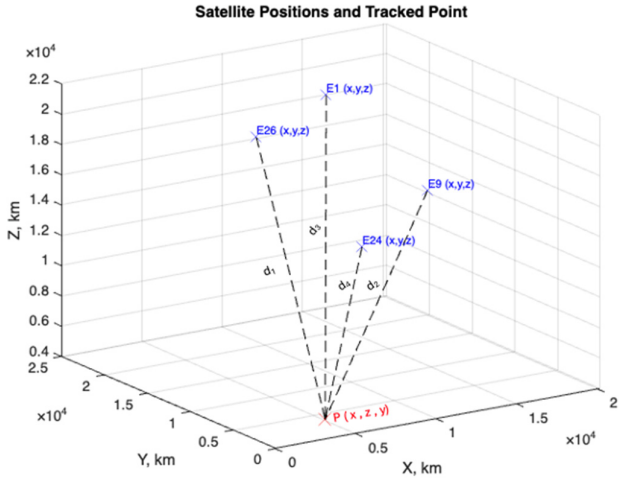


Figure 10. Positions of the Galileo system satellites and the user's receiver in the geocentric coordinate system. Variant number 2.

From Figure 4, we can conclude that even minor errors Δd_{i-E} significantly impact the accuracy of determining ΔP. If the errors Δd_{i-E} varied from −5.0 cm to 9.0 cm, then the error ΔP was from 0 to 1.2 m. Next, we changed the value of l and determined the coordinates' errors ΔX, ΔY, ΔZ, and ΔP.

Figure 5 shows the simulation results for l = 0.08. If the constant k was equal to 0.08, the errors ΔX, ΔY, and ΔZ varied from −0.2 m to 0.2 m, while the errors ΔP ranged from 0 to 4.9 m.

Figure 6 shows the simulation results for l = 0.2. If the constant l was equal to 0.2, the errors ΔX, ΔY, and ΔZ varied from −0.5 m to 0.5 m, while the errors ΔP ranged from 0 to 11.8 m. We have gradually checked the errors ΔP for more significant errors Δd_{i-E}. The simulation results confirmed that if the Δd_{i-E} error increases, the accuracy of determining

the position of the user's receiver deteriorates. This is due to the method of calculating the position of the user's receiver, which requires the user to know the exact position of the satellites and his distance from cooperating satellites. Figure 7 shows the mean values (MVs) of the receiver's position determination errors (PDEs) mΔP depending on the constant l.

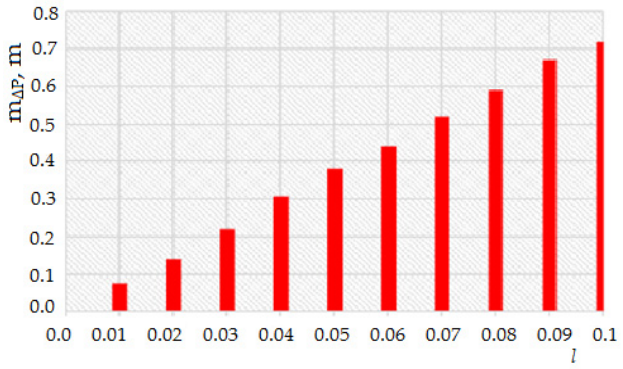


Figure 11. The MVs of the receiver's PDEs mΔP depend on the constant l. Variant no. 2.

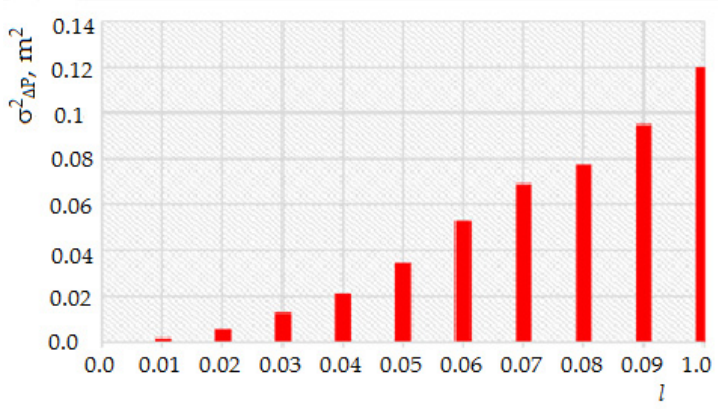


Figure 12. The MSD of the receiver's PDEs depends on the constant l. Variant no. 2.

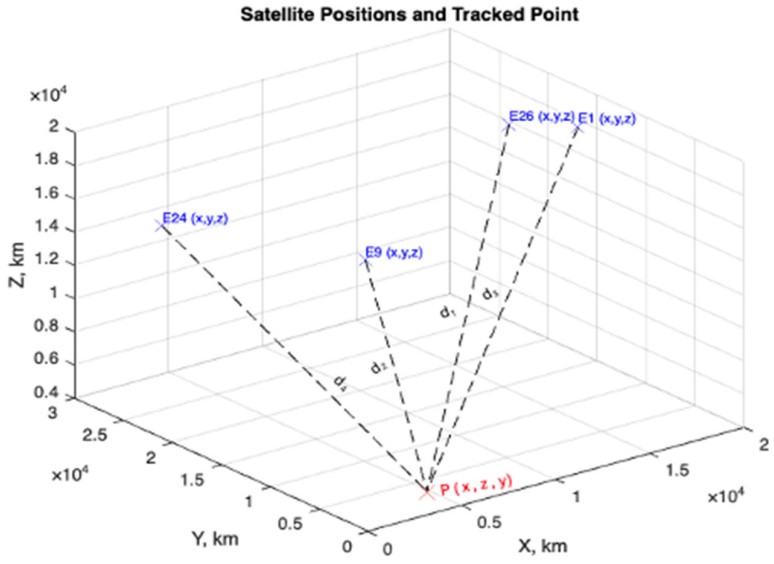


Figure 13. Positions of the Galileo system satellites and the user's receiver in the geocentric coordinate system. Variant number 3.

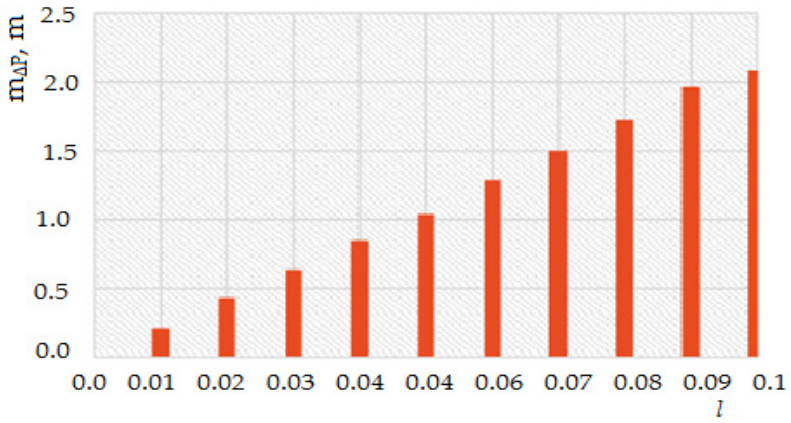


Figure 14. The MVs of the receiver's PDEs $m_{\Delta P}$ depending on the constant*l*. Variant no. 3.

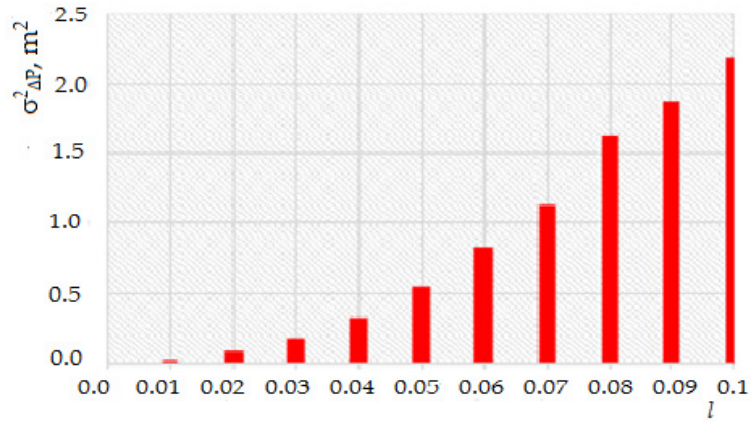


Figure 15. The MSD of the receiver's PDEs $\sigma^2{}_{\Delta P}$ depends on the constant l. Variant no. 3.

Calculations confirmed that as Δd_{i-E} (depends on k) increased, the MVs of the receiver's PDEs $m_{\Delta P}$ increased. During the simulations, l was changed from 0 to 0.1, corresponding to the errors Δd_{i-E} from −0.4 m to 0.25 m. The MVs of the receiver's PDEs $m_{\Delta P}$ varied from 1.94×10^{-8} m to 1.69 m. The mean square deviation (MSD) of the receiver's PDEs depending on the constant l is shown in Figure 8.

Even in this case, calculations confirmed that as Δd_{i-E} (depends on k) increased, the MSD value of the receiver's PDEs $\sigma^2{}_{\Delta P}$ also increased. During the simulations, the constant k was changed from 0 to 0.1, and the mean square deviation value of the receiver's positioning error varied from 2.74×10^{-46} m^2 to 1.22 m^2.

Figure 9 shows the MVs of the receiver's PDEs $m_{\Delta P}$ depending on the constant $l = 0.1$ to 1.0. The simulation confirmed that distance measurement errors significantly impact the user's receiver's PDEs. The values of $m_{\Delta P}$ ranged from 1.47 m to 15.0 m.

We observed how the value of the PDEs of the receiver's P depends on the position of the Galileo system satellites. The positions of the Galileo satellites were randomly selected to be visible to the user's receiver. We called this experiment variant number 2. The position of the Galileo system satellites according to variant number 2 is shown in Figure 10.

The coordinates of the Galileo system satellites according to variant number 2 are listed in Table 3. The date is 31 December 2023, at 03:18:26 pm. We chose the same simulation conditions as for variant 1, to compare the results.

Table 3. Coordinates of the Galileo system satellites and the user's receivers. Variant number 2.

Name	X, m	Y, m	Z, m
GSAT0203 (E26)	10,379,917.0	21,718,209.0	17,229,827.0
GSAT0205 (E24)	11,532,457.0	11,532,457.0	12,223,933.0
GSAT0209 (E9)	20,231,485.0	20,231,485.0	12,113,692.0
GSAT0210 (E1)	12,293,393.0	17,140,283.0	20,762,710.0
ARP KSC + 300.0 m	3,934,235.0	1,529,238.0	4,766,291.0

First, we investigated the PDEs of the user's receiver, provided that the receiver has the coordinates of visible satellites and the exact distances to these satellites available. The MVs and the mean square deviation of errors in the coordinates of the user's receiver P for variant no. 2 and $l = 0.0$ have been meticulously analyzed and are presented in Table 4.

Table 4. MVs m_Δ and variance σ^2_Δ of user P coordinate errors.

Name	ΔX, m	ΔY, m	ΔZ, m
m_Δ,m	-6.5192×10^{-9}	-2.5611×10^{-9}	9.3132×10^{-10}
$\sigma^2{}_\Delta$, m^2	0.0	0.0	0.0

Calculations have shown that if we have the correct coordinates of the Galileo satellites and the exact distances of the user's receiver from these satellites, the Galileo system will accurately determine the receiver's position. Figure 11 shows the MVs of the receiver's PDEs depending on the constant l.

In this case, calculations confirmed that as Δd_{i-E} increased, the MVs of the receiver's PDEs $m_{\Delta P}$ increased as well. During the simulations, the constant l was changed from 0 to 0.1, corresponding to the errors Δd_{i-E} from -0.4 m to 0.25 m. The MVs of the PDEs $m_{\Delta P}$ varied from 1.06×10^{-7} m to 0.72 m. The MSD of the receiver's PDEs $\sigma^2{}_{\Delta P,}$ depending on the constant l, is shown in Figure 12.

We performed simulations to determine the position of the user's receiver P using the Galileo system according to variant number 2. The simulations show that with the increase in the Δd_{i-E}, the MSD of the receiver's position determination error increased. During the simulations, the constant l was changed from 0 to 0.1, and the mean square deviation value of the receiver's positioning error varied from 2.74×10^{-46} m^2 to 0.12 m^2.

Another experiment was carried out to check how the PDEs of the user's receiver depends on the constellation of the Galileo system satellites, which we called variant number 3. The coordinates of satellites according to variant number 3 are shown in Figure 13.

The coordinates of the Galileo system satellites, specifically for variant number 3, are detailed in Table 5, dated 12 June 2023, at UTC 06:40:02 am. These data are crucial as it forms the basis for our evaluation of the Galileo system's accuracy in determining the position of the user's receiver P, assuming P has access to the precise coordinates of visible satellites and their respective distances. In this scenario, the constant $l = 0$.

Table 6 shows the MVs and MSD errors for determining the coordinates of the user's receiver P for variant no. 3 and $l = 0.0$.

Also, in this case, the Galileo system correctly determines the user's position based on the actual location of the Galileo system satellites and the precise distances of the user's receiver to these satellites. Next, further simulations were performed, in which the constant l had values from 0.0 to 0.1. Figure 14 shows the MVs of the receiver's PDEs $m_{\Delta P}$ depending on the constant k.

Table 5. Coordinates of Galileo system satellites and the user's receiver. Variant no. 3.

Name	X, m	Y, m	Z, m
GSAT0203 (E26)	15,808,595.0	15,954,099.0	19,285,449.0
GSAT0205 (E24)	2,328,508.0	25,483,057.0	14,835,096.0
GSAT0209 (E9)	12,821,768.0	24,872,048.0	9,673,128.0
GSAT0210 (E1)	18,217,144.0	13,516,486.0	19,013,602.0
ARP KSC + 300.0 m	3,934,235.0	1,529,238.0	4,766,291.0

Table 6. MVs m_Δ and variance σ^2_Δ of user P coordinate errors.

Name	ΔX, m	ΔY, m	ΔZ, m
m_Δ,m	-1.30×10^{-8}	-3.80×10^{-8}	-2.60×10^{-8}
$\sigma^2{}_\Delta$, m^2	0.0	0.0	0.0

Figure 14 shows that if the error Δd_{i-E} increased (increasing the constant l), the $m_{\Delta P}$ increased. If l = 0 to 0.1, which corresponds to the errors Δd_{i-E} from −0.4 m to 0.25 m, the MVs of the receiver's PDEs $m_{\Delta P}$ varied from 4.86×10^{-8} m to 2.09 m. The dispersion of the receiver's position determination errors depending on the constant k is shown in Figure 15.

Even with the position of the Galileo system satellites according to variant 3, the simulation results confirmed that the increase in the Δd_{i-E} increased the dispersion of the receiver's position determination error. During the simulations, the constant l = 0 to 0.1 and the mean square deviation value of the receiver's positioning error varied from 1.43×10^{-44} m^2 to 2.18 m^2.

Table 7 shows the MVs m_P and MSD σ^2_P errors for determining the coordinates of the user's receiver P for variants 1 to 3 and l = 0.0 to 0.1. We chose three variants of the satellite's location. Each variant was selected on a different day and time. The simulation conditions were the same for each variant. The results of the accuracy comparison are shown in the following tables.

Table 7. Mean values m_P and MSD σ^2_P of errors position of receiver P. Variants 1 to 3.

Variant No.	$m_{\Delta P}$, m		$\sigma^2{}_{\Delta P}$, m^2		$m_{\Delta X}$, m		$m_{\Delta Y}$, m		$m_{\Delta Z}$, m	
	l = 0.0	l = 0.1	l = 0.0	l = 0.1	l = 0.0	l = 0.1	l = 0.0	l = 0.1	l = 0.0	l = 0.1
1.	1.9×10^{-8}	1.69	2.7×10^{-46}	1.22	-1.8×10^{-8}	−0.15	-8.6×10^{-9}	0.063	1.8×10^{-9}	−0.024
2.	7.0×10^{-9}	0.72	2.4×10^{-46}	0.12	-6.5×10^{-9}	−0.014	-2.5×10^{-9}	−0.009	9.3×10^{-10}	−0.004
3.	4.8×10^{-8}	2.09	1.9×10^{-44}	2.18	-1.3×10^{-8}	0.035	-3.8×10^{-8}	0.074	-2.6×10^{-8}	0.033

Research has confirmed the fact that the position of the Galileo satellites affects the system's ability to determine the user's position. Tables 7 and 8 clearly show that with the same simulation conditions and different positions of the satellites, the errors in measuring the position user P were not approximately the same.

Table 8. Maximum errors of determining the coordinates and position of receiver P. Variants 1 to 3.

Variant No.	l = 0.1			
	ΔX_{max}, m	ΔY_{max}, m	ΔZ_{max}, m	ΔP_{max}, m
1.	5.2	2.04	−1.5	5.9
2.	−1.8	1.1	1.5	2.2
3.	7.8	−6.3	−4.2	7.8

The research results shown in Figures 3 to 15 and Table 7 show that the errors Δd_{i-E} significantly affect the accuracy of the determination of receiver P. It was verified that distance measurement errors between 0.05 and 0.09 m caused positioning errors ΔP of up to 1.2 m. The simulation confirmed that determining the quality of the user's receiver using the mean value of the receiver's positioning error is inappropriate. Errors may occur in individual measurements of the receiver's position, which are several times greater than the mean value of the user's receiver's PDEs. For example, in variant number 3, for l = 0.1, the MV of the X-coordinate determination error is $\Delta X = 3.50 \times 10^{-2}$ m. Still, the maximum X-coordinate determination error was equal to 7.08 m (see Tables 7 and 8).

4. Conclusions

Current trends in the research of satellite navigation systems confirm that they are important in air transport. High demands are placed on the quality of services provided by the Galileo system. Our research aimed to find out what influence the accuracy of determining the distance between the Galileo system user's receiver and cooperating satellites d_{i-E} has on the ability to determine the position of the user P. The user's receiver position measurement model was developed using Groebner's algebraic approaches.

When creating distance measurement error models between the Galileo system user's receiver and cooperating satellites, we assumed that the values of these errors consider all factors that affect the accuracy of these distance measurements. Determining the relationship between the accuracy of the receiver-to-satellite distance measurement and the accuracy of the user's receiver positioning allows new methods to be developed to achieve greater accuracy when determining the position result.

To evaluate the algorithms mentioned, we used a statistical file containing the results of 500 simulations of determining user P's location. These results determined the absolute, MV, and MSD errors monitored parameters. Suppose the distances d_{i-E} were measured accurately, errors ΔX, ΔY, and ΔZ ranged from 1.86×10^{-9} m to -1.86×10^{-8} m. These errors should be equal to zero and were caused by a numerical error in the calculation due to the software used. In our contribution, we determined the requirements for the accuracy of the distance measurement between the Galileo system user's receiver and the satellites that determine its position.

For example, if the absolute errors of measuring the distance d_{i-E} varied from −0.05 m to 0.09 m, the absolute error ΔP ranged from 0 to 1.2 m. In the case of variant number one, if the constant l = 0.01 to 0.1, then the MVs of the receiver's PDEs ranged between 0.14 m and 1.69 m. The mean square deviation of the PDEs receiver varied from 0.01 m^2 to 1.22 m^2. In the case of variant number three, if the constant l = 0.01 to 0.1, then the MVs of the PDEs receiver ranged from 0.21 m to 2.09 m. The mean square deviation of the PDEs receiver varied from 0.02 m^2 to 2.18 m^2.

The simulation results confirmed that the data on the accuracy of determining the coordinates of the user's receiver of the Galileo system must be treated very carefully, especially if it is a mean error value. In the following research, we will solve the problem of reducing the telemetry method's sensitivity to errors in measuring d_{i-E} when determining the position of the satellite navigation system user's receiver.

Author Contributions: Conceptualization M.D. and S.Č.; data curation, M.D. and S.Č.; methodology M.D., S.Č. and L.M., formal analysis S.Č. and L.M.; validation M.D., S.Č. and L.M.; supervision M.D. and L.M.; resources M.D. and L.M.; writing—original draft preparation M.D., S.Č. and L.M.; writing—review and editing S.Č. and L.M. All authors have read and agreed to the published version of the manuscript.

Funding: This research received no external funding.

Institutional Review Board Statement: Not applicable.

Informed Consent Statement: Not applicable.

Data Availability Statement: Data are contained within the article.

Conflicts of Interest: The authors declare no conflicts of interest.

References

1. Hein, G.W. Status, Perspectives and Trends of Satellite Navigation. *Satell. Navig.* **2020**, *1*, 22. [CrossRef] [PubMed]
2. Švehla, D. *Geometrical Theory of Satellite Orbits and Gravity Field*; Springer: Berlin/Heidelberg, Germany, 2018.
3. Michalski, A.; Czajewski, J. Instrumentatio Nnotes-The Accuracy of the Global Positioning Systems. *IEEE Instrum. Meas. Mag.* **2004**, *7*, 56–60. [CrossRef]
4. Kong, T.; Ma, L.; Ai, G. Research on Improving Satellite Positioning Precision Based on Multi-Frequency Navigation Signals. *Sensors* **2022**, *22*, 4210. [CrossRef] [PubMed]
5. Rychlicki, M.; Kasprzyk, Z.; Rosiński, A. Analysis of Accuracy and Reliability of Different Types of GPS Receivers. *Sensors* **2020**, *20*, 6498. [CrossRef]
6. Li, T.; Zhang, H.; Gao, Z.; Chen, Q.; Niu, X. High-Accuracy Positioning in Urban Environments Using Single-Frequency Multi-GNSS RTK/MEMS-IMU Integration. *Remote Sens.* **2018**, *10*, 205. [CrossRef]
7. Li, X.; Gou, H.; Li, X.; Shen, Z.; Lyu, H.; Zhou, Y.; Wang, H.; Zhang, Q. Performance Analysis of Frequency-Mixed PPP-RTK Using Low-Cost GNSS Chipset with Different Antenna Configurations. *Satell. Navig.* **2023**, *4*, 26. [CrossRef]
8. Wang, J.; Li, Q.; Liu, R. Improvement of Positioning Accuracy with GNSS Using User Range Accuracy and Posterior Variance Model. In Proceedings of the Satellite Division's International Technical Meeting 2019, Miami, FL, USA, 16–20 September 2019. [CrossRef]
9. Ferre, R.M.; Richter, P.; Falletti, E.; De La Fuente, A.; Lohan, E.S. A Survey on Coping with Intentional Interference in Satellite Navigation for Manned and Unmanned Aircraft. *IEEE Commun. Surv. Tutor.* **2020**, *22*, 249–291. [CrossRef]
10. Qiao, J.; Lu, Z.; Lin, B.; Song, J.; Xiao, Z.; Wang, Z.; Li, B. A Survey of GNSS Interference Monitoring Technologies. *Front. Phys.* **2023**, *11*, 1133316. [CrossRef]
11. Morrison, A.; Sokolova, N.; Gerrard, N.; Rødningsby, A.; Rost, C.; Ruotsalainen, L. Radio-Frequency Interference Considerations for Utility of the Galileo E6 Signal Based on Long-Term Monitoring by ARFIDAAS. *Navig. J. Inst. Navig.* **2023**, *70*, navi.560. [CrossRef]
12. Dutta, P.; Halder, T.; Banerjee, S.; Basak, A.; Nanda, S.; Chakravarty, D. Analysis of Jamming and Anti Jamming Techniques for Galileo GNSS. *Mater. Today Proc.* **2022**, *58*, 489–495. [CrossRef]
13. Arribas, J.; Vilà-Valls, J.; Ramos, A.L.L.; Fernández-Prades, C.; Closas, P. Air Traffic Control Radar Interference 505Event in the Galileo E6 Band: Detection and Localization. *Navig. J. Inst. Navig.* **2019**, *66*, 505–522. [CrossRef]
14. Zhang, J.; Lohan, E.S. Effect of Narrowband Interference on Galileo E1 Signal Receiver Performance. *Int. J. Navig. Obs.* **2011**, *2011*, 959871. [CrossRef]
15. Bahadur, B. Real-Time Single-Frequency Precise Positioning with Galileo Satellites. *J. Navig.* **2021**, *75*, 124–140. [CrossRef]
16. Liu, T.; Chen, Q.; Geng, T.; Jiang, W.; Chen, H.; Zhang, W. The Benefit of Galileo E6 Signals and Their Application in the Real-Time Instantaneous Decimeter-Level Precise Point Positioning with Ambiguity Resolution. *Adv. Space Res.* **2022**, *69*, 3319–3332. [CrossRef]
17. Yalvaç, S. Investigating the Historical Development of Accuracy and Precision of Galileo by Means of Relative GNSS Analysis Technique. *Earth Sci. Inform.* **2021**, *14*, 193–200. [CrossRef]
18. Fernández-Hernández, I.; Chamorro-Moreno, A.; Cancela-Diaz, S.; Calle-Calle, J.D.; Zoccarato, P.; Blonski, D.; Senni, T.; De Blas, F.J.; Hernández, C.; Simón, J.; et al. Galileo High Accuracy Service: Initial Definition and Performance. *GPS Solut.* **2022**, *26*, 65. [CrossRef]
19. De Blas, F.J.; Vázquez, J.L.; Ramos-Hernández, C.; Ostolaza, J.; Lagrasta, S.; Fernández-Hernández, I.; Blonski, D. The Galileo High Accuracy Service (HAS): A Pioneer Free-of-Charge Global Precise Positioning Service. In Proceedings of the Satellite Division's International Technical Meeting, Denver, CO, USA, 11–15 September 2023. [CrossRef]
20. Luo, X.; Schaufler, S.; Branzanti, M.; Chen, J. Assessing the Benefits of Galileo to High-Precision GNSS Positioning–RTK, PPP and Post-Processing. *Adv. Space Res.* **2021**, *68*, 4916–4931. [CrossRef]
21. Martini, I.; Susi, M.; Cucchi, L.; Fernandez-Hernandez, I. Galileo high accuracy service performance and anomaly mitigation capabilities. *GPS Solut.* **2024**, *28*, 25. [CrossRef]
22. Averyanova, Y.; Kutsenko, O.; Konin, V. Interference Suppression at Cooperative Use of GPS, GLONASS, GALILEO, BEIDOU. In Proceedings of the 2020 IEEE Ukrainian Microwave Week (UkrMW), Kharkiv, Ukraine, 21–25 September 2020. [CrossRef]
23. Islam, S.; Bhuiyan, M.Z.H.; Thombre, S.; Kaasalainen, S. Combating Single-Frequency Jamming through a Multi-Frequency, Multi-Constellation Software Receiver: A Case Study for Maritime Navigation in the Gulf of Finland. *Sensors* **2022**, *22*, 2294. [CrossRef]
24. Zalewski, P.; Bilewski, M. GNSS Measurements Model in Ship Handling Simulators. *IEEE Access* **2019**, *7*, 76428–76437. [CrossRef]
25. Garcia-Fernandez, M.; Hoyas-Ester, I.; Lopez-Cruces, A.; Siutkowska, M.; Banqué-Casanovas, X. Accuracy in WiFi Access Point Position Estimation Using Round Trip Time. *Sensors* **2021**, *21*, 3828. [CrossRef]
26. Awnage, J.L.; Grafarend, E.W. *Solving Algebraic Computational Problems in Geodesy and Geoinformatics*; Kap. 9.2, Ranging by Global Positioning System; Springer: Berlin/Heidelberg, Germany, 2004; pp. 107–116. ISBN 3-540-23425-X.

27. Džunda, M.; Hrban, A. Accuracy of the Passive Tracking Systems. In Proceedings of the 12th International Conference on Microwaves and Radar. MIKON-98, Conference Proceedings (IEEE Cat. No.98EX195), Krakow, Poland, 20–22 May 1998. [CrossRef]
28. Džunda, M.; Kotianová, N.; Dzurovčin, P.; Szabo, S.; Jenčová, E.; Vajdová, I.; Koščák, P.; Liptáková, D.; Hanák, P. Selected Aspects of Using the Telemetry Method in Synthesis of RelNav System for Air Traffic Control. *Int. J. Environ. Res. Public Health* **2020**, *17*, 213. [CrossRef]

Disclaimer/Publisher's Note: The statements, opinions and data contained in all publications are solely those of the individual author(s) and contributor(s) and not of MDPI and/or the editor(s). MDPI and/or the editor(s) disclaim responsibility for any injury to people or property resulting from any ideas, methods, instructions or products referred to in the content.